Table 1. Martian atmospheric model. Surface pressure, 7 mbar.

| Altitude (km) | Temp. (°K) | Density ($cm^{-3}$) | | |
|---|---|---|---|---|
| | | $CO_2$ | O | CO |
| 0 | 220 | $2 \times 10^{17}$ | | |
| 50 | 160 | $1 \times 10^{15}$ | | |
| 100 | 160 | $2 \times 10^{12}$ | $3 \times 10^{10}$ | $3 \times 10^{10}$ |
| 150 | 180 | $4.6 \times 10^{9}$ | $2 \times 10^{9}$ | $6 \times 10^{8}$ |
| 200 | 320 | $2.5 \times 10^{7}$ | $2 \times 10^{8}$ | $2.2 \times 10^{7}$ |
| 250 | 400 | $2.4 \times 10^{5}$ | $7 \times 10^{7}$ | $1.6 \times 10^{6}$ |

gas density near 125 km would be close to $10^{11}$ molecules per cubic centimeter. In such a case the maximum in the photoionization rate would occur there when the sun is 20 degrees above the horizon. Hence there is a good possibility that the ionosphere is an F1 region. Since the ionization rate would be about $1.2 \times 10^3$ $cm^{-3}$ $sec^{-1}$ at the maximum, the electron density would be $9 \times 10^4$ $cm^{-3}$ (as observed) if the effective recombination coefficient were $1.5 \times 10^{-7}$ $cm^3$ $sec^{-1}$. This would correspond to the expected value for $O_2^+$ and could mean that this ion is the one predominantly formed as a result of ion-molecule reactions.

The suppression of an F2 peak can readily occur if the rate coefficient for

$$O^+ + CO_2 \rightarrow CO + O_2^+ \qquad (1)$$

is indeed $1.2 \times 10^{-9}$ $cm^3$ $sec^{-1}$ (*4*). It is only necessary in that case that the ratio of the O to $CO_2$ density remain less than $10^2$ up to the altitude at which diffusion loss of $O^+$ begins to compete with chemical loss. The reason is that the rate of ionization of atomic oxygen in the optically thin regions of the Martian upper atmosphere is given by

$$Q(O) = 1.3 \times 10^{-7} n(O) \qquad (2)$$

Below the altitude at which diffusion becomes important the steady state condition for creation and loss of $O^+$ is

$$Q(O) = 1.2 \times 10^{-9} n(CO_2)\, n(O^+) \qquad (3)$$

Hence

$$n(O^+) = 10^2 n(O)/n(CO_2) \qquad (4)$$

To avoid an F2 build-up of $O^+$ to densities greater than $10^4$ $cm^{-3}$ it is required that the condition

$$n(O)/n(CO_2) \leqq 10^2 \qquad (5)$$

hold up to the altitude at which

$$1.2 \times 10^{-9} n(CO_2) = D(O^+)/H^2(O) \qquad (6)$$

where $D$ is the ambipolar diffusion coefficient for $O^+$ in O and $H$ is the scale height of atomic oxygen (presumed to be the major constituents). If $H(O)$ is 50 km, this condition requires that at the altitude where the $CO_2$ density is given by

$$n(CO_2) = 3 \times 10^{11}/n(O) \qquad (7)$$

the condition (Eq. 5) be satisfied. Hence at that altitude

$$n(CO_2) = 1.7 \times 10^6 \text{ cm}^{-3} \qquad (8)$$

and

$$n(O) \leqq 1.7 \times 10^8 \text{ cm}^{-3} \qquad (9)$$

In the adopted model this $CO_2$ density is attained at about 230 km. From the upper limit to the oxygen density there, the maximum density at other altitudes is determined, diffusive separation being assumed. Presumably O and CO are equally abundant near 100 km. The outlines of the resultant atmospheric model are sketched in Table 1. In the model there is only modest dissociation of $CO_2$, but diffusive separation could occur. As Chamberlain and McElroy point out, formation of $O_2$ near 100 km will shield $CO_2$ from dissociating radiation and the low level of $CO_2$ dissociation is not therefore unreasonable. Presumably, then, $O_2$ must be present to an abundance of at least $10^{11}$ $cm^{-3}$ at 100 km.

*Note added in proof*: Belton and Hunten (*5*) have determined with precision the partial pressure of $CO_2$, the surface pressure, and temperature spectroscopically. A pure $CO_2$ atmosphere with surface pressure 6 mbar and temperature 220°K is consistent with their measurement.

T. M. DONAHUE

*University of Pittsburgh,*
*Pittsburgh, Pennsylvania*

### References and Notes

1. J. W. Chamberlain and M. B. McElroy, *Science* **152**, 21 (1966).
2. A. Kliore, D. L. Cain, G. S. Levy, V. R. Eshleman, G. Fjelbo, *ibid.* **149**, 1243 (1965).
3. F. S. Johnson, *ibid.* **150**, 1445 (1965).
4. F. F. Fehsenfeld, A. L. Schmeltekopf, and E. E. Ferguson, *J. Chem. Phys.* **4**, No. 8 (1966).
5. M. J. S. Belton and D. M. Hunten, *Astrophys. J.*, in press.

6. Supported in part by the Atmospheric Sciences Section (Aeronomy), NSF, and by NASA contract NASr-179. I thank J. W. Chamberlain and M. B. McElroy for criticism, discussion, and access to their manuscript before publication.

15 March 1966

---

## Radiocarbon Chronology of Late Pleistocene Deposits in Northwest Washington

Abstract. *Fourteen radiocarbon dates of shells and wood from late Pleistocene sediments in northwest Washington provide evidence for correlation of the Everson interstadial with the Two Creeks interval of the midcontinent and suggest possible correlations between the Sumas and Valders stadials and between the Vashon stadial and part of the Tazewell-Cary advances.*

The latest Pleistocene deposits of the Fraser Glaciation in northwest Washington, in order of decreasing age, consist of (i) till and associated drift of the Vashon stadial, (ii) glaciomarine drift and related sediments of the Everson interstadial, and (iii) glacial drift of the Sumas stadial. This paper focuses attention on the radiocarbon chronology of the Everson interstadial, relationships of the Everson interstadial to the age of the Vashon and Sumas stadials, and possible correlations between late Pleistocene events in Washington and those in the midcontinent region and Rocky Mountains.

The presence of marine shells in late Pleistocene deposits in parts of Puget lowland of northwest Washington was noted by Reagan (*1*) and Bretz (*2*) near the early part of this century, but the origin of these deposits was not clear until Armstrong and Brown (*3*) suggested that similar fossiliferous sediments in southwestern British Columbia were deposited from floating ice in a marine environment. The origin of late Pleistocene fossiliferous marine deposits in northwest Washington has been discussed in an earlier paper (*4*), and these sediments have been included in the Everson interstadial by Armstrong, Crandell, Easterbrook, and Noble (*5*). Correlative deposits have now been traced over a large area in the Puget lowland and San Juan Islands, and 14 radiocarbon dates have been obtained from shells, wood, and peat in the deposits.

Distribution of the radiocarbon samples is shown in Fig. 1. The total area encompassed by the deposits is now known to exceed 3000 square miles (7700 $km^2$). Correlative deposits to the north in British Columbia span a similar area (Armstrong and others, *5*). Thus, these late Pleistocene glacial deposits constitute a unit of significant importance in the deglaciation of northwest Washington. Relative abundance of shells, wood, and peat in the deposits provides an opportunity for establishment of their age by radiocarbon dating. The total range of the radiocarbon dates is from 10,370 ± 300 to 13,010 ± 170 years ago (Table 1), but whether or not this range represents the true total age range of the deposits is uncertain at present. The oldest sample, dated at 13,010 ± 170 years (sample UW-32), comes from a section between localities where ages of 11,850 ± 240 and 12,535 ± 300 years were obtained from samples in the same stratigraphic position in the same depositional unit. The 13,010 year date was originally reported as 10,200 ± 110 but was later corrected for radon contamination of the hydrogen used for making methane gas for counting. The lowest age determination, 10,370 years (sample I-1035), is from wood in glaciomarine drift and, although other dates from the same unit are somewhat older, there is no reason to doubt the date. The dates from wood in the glaciomarine drift may represent a time slightly earlier than the arrival of the ice at the locality, since the wood had to be transported to the site of deposition. The dates for the shells should be contemporaneous with the deposit, as inferred from their preservation described in an earlier paper (*4*). Considering the accuracy of the radiocarbon dating method and the number of determinations made to date, the best estimate for the time span of dep-

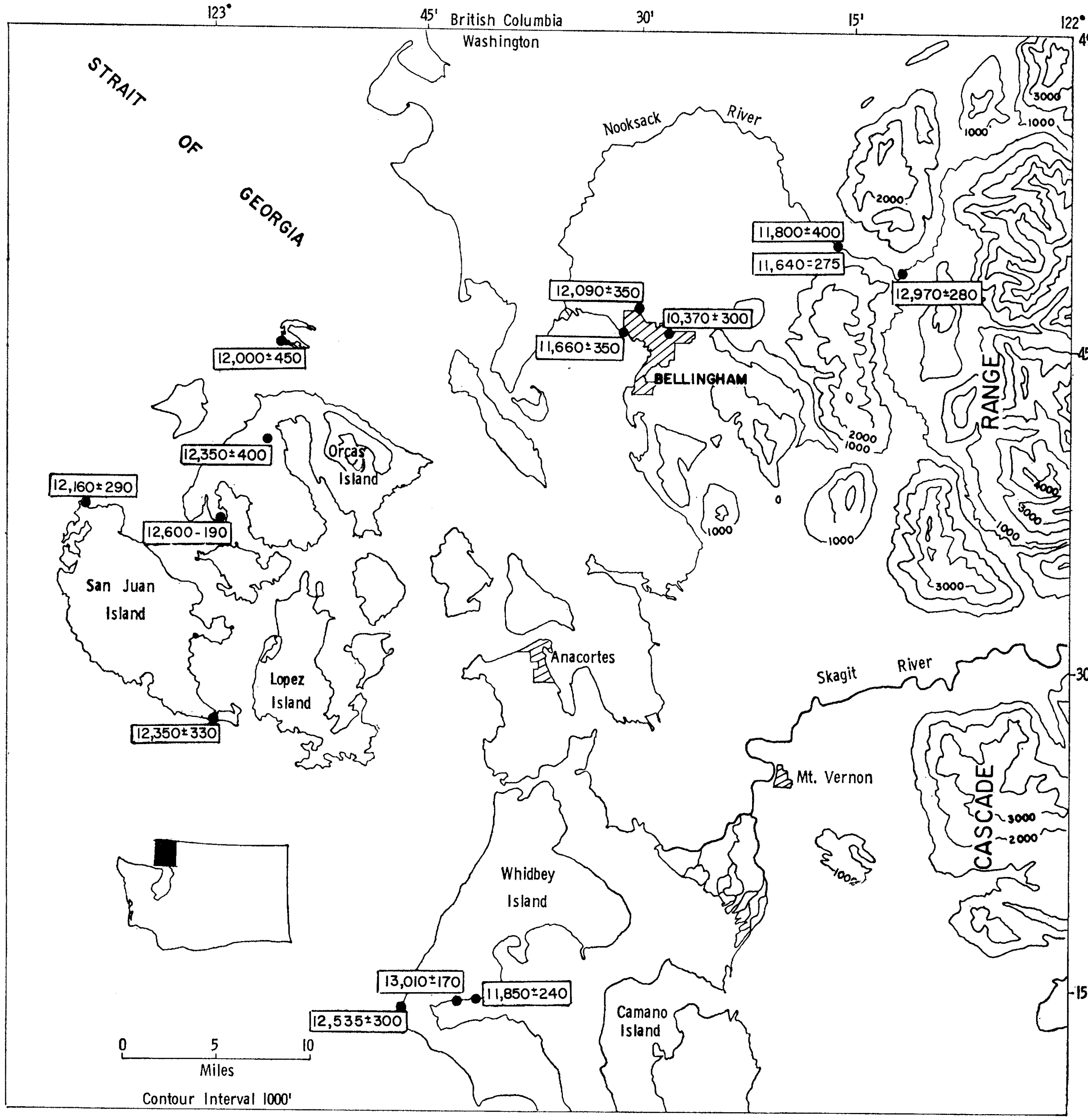

Fig. 1. Distribution of radiocarbon-dated samples from late Pleistocene deposits in northwest Washington.

Table 1. Summary of radiocarbon dates. Ages in years before 1950.

| Age (years) | Sample No.* | Material | Stratigraphic position |
|---|---|---|---|
| 10,370 ± 300 | I-1035 | Wood | From glaciomarine drift |
| 11,640 ± 275 | W-940 | Peat | Within glaciomarine sequence |
| 11,660 ± 350 | W-996 | Shells | From glaciomarine drift |
| 11,800 ± 400 | I-1037 | Wood | From glaciomarine drift |
| 11,850 ± 240 | I-1448 | Shells | From glaciomarine drift |
| 12,000 ± 450 | I-1471 | Shells | From glaciomarine drift |
| 12,090 ± 350 | W-984 | Peat | Within glaciomarine sequence |
| 12,160 ± 290 | I-1470 | Shells | From glaciomarine drift |
| 12,350 ± 330 | I-1469 | Shells | From glaciomarine drift |
| 12,350 ± 400 | I-969 | Shells | From glaciomarine drift |
| 12,535 ± 300 | I-1079 | Shells | From glaciomarine drift |
| 12,600 ± 190 | I-1881 | Shells | From glaciomarine drift |
| 12,970 ± 280 | I-1447 | Shells | From glaciomarine drift |
| 13,010 ± 170 | UW-32 | Shells | From glaciomarine drift |

* Prefix denotes laboratory where sample was analyzed: I, Isotopes, Inc.; W, U.S. Geological Survey; UW, University of Washington.

osition is approximately 2500 years.

In the northern part of region shown in Fig. 1, two glaciomarine units separated by nonmarine peat and sand are present, both lying within the 2500-year span discussed above. However, in the San Juan Islands (west edge of Fig. 1) and in the southern half of the region shown in Fig. 1 only one glaciomarine unit is present. Whether the single unit in the southern and western parts of the area represents the equivalent of one of the two units or spans, the time of deposition of both units is not clearly demonstrable at present. The latter possibility appears more probable on the basis of present evidence.

The glaciomarine drifts from which the 14 radiocarbon dates were obtained are all included within the Everson interstadial of the Fraser Glaciation and represent a phase during the deglaciation of the last major glaciation in northwest Washington and southwest British Columbia.

The age limits for the Everson interstadial define the upper age of the Vashon stadial and the lower age of the Sumas stadial. However, since these age boundaries are for geologic climate units which are time-transgressive, the straight boundaries between intervals shown in Fig. 2 would not be isochronous if plotted against latitude.

A comparison of the late Pleistocene chronology of the Puget lowland with that of the mid-continent and Rocky Mountain regions is shown in Fig. 2. Leighton (*6*) recognized several subdivisions of the Wisconsin glaciation, including five glacial episodes within the approximate time span of the Fraser Glaciation in northwest Washington. These include, from oldest to youngest, the Iowan, Tazewell, Cary, Mankato, and Valders. Frye and Willman (*7*) grouped four of the pre-Two Creeks subdivisions into one glacial episode which they referred to as the Woodfordian. Chronology of glacial events in the Rocky Mountain region is hampered by a paucity of radiocarbon dates, but a generalized correlation has been inferred by Richmond (*8*).

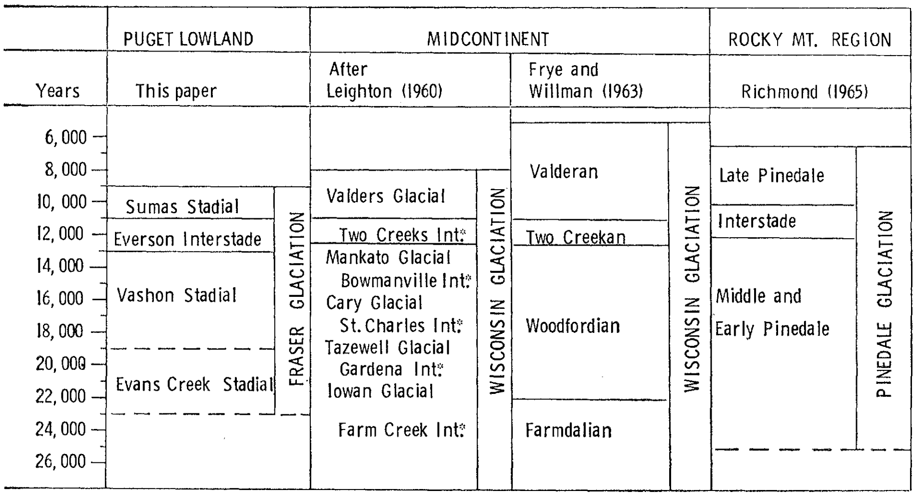

Fig. 2. Correlation of late Pleistocene chronology of northwest Washington with the midcontinent and Rocky Mountain regions.

Comparison of the late Pleistocene radiocarbon chronologies shown in Fig. 2 suggests a correlation between the Everson interstadial and the Two Creeks intraglacial of the mid-continent. Possible correlation of the Everson interstadial with the interstadial between the late and middle Pinedale stadials in the Rocky Mountains is considerably more tenuous because of the lack of radiocarbon dates in the Rockies. A correlation is also suggested between the Sumas, Valders, and late Pinedale stadials. However, the Sumas stadial ended prior to 9000 years ago and thus may represent only the early part of the Valders. Correlation of the Sumas stadial with the late Pinedale stadial seems logical but the lack of datable material in the Pinedale makes the correlation somewhat tentative.

The maximum ice advance of the Fraser Glaciation occurred during the Vashon. Mullineaux, Waldron, and Rubin (*9*) have obtained radiocarbon dates of 15,000 ± 400 years (sample W-1227) and 15,000 ± 300 years (sample W-1305) from deposits beneath Vashon till in Seattle, indicating that the Vashon advance is younger than about 15,000 years in the Seattle area.

The youngest pre-Vashon radiocarbon dates farther north range from 19,150 ± 250 (sample GSC-195) to 35,400 ± 400 years (sample GSC-202) in southwest British Columbia (*5, 10*). Thus Vashon ice advanced southward across the U.S.–Canadian border sometime after 19,000 years ago, but how much later is at present not certain. The Vashon stadial terminated about 13,000 years ago with the advent of glaciomarine conditions in the lowland. The Vashon maximum appears to correlate with the Cary of the mid-continent and may encompass part of the Tazewell. It would correspond to part of the Woodfordian of Frye and Williams (*7*). Relative to Rocky Mountain terminology the Vashon appears to be equivalent to the middle stadial of the Pinedale Glaciation but might also include all or part of the early Pinedale. Another possibility is that the early Pinedale may be equivalent to the Evans Creek stadial.

D. J. EASTERBROOK
*Department of Geology, Western Washington State College, Bellingham*

## References and Notes

1. A. B. Reagan, *Kansas Acad. Sci. Trans.* **255**, pt. 3, 95–121 (1907).
2. J. H. Bretz, *Wash. Div. Mines Geol. Bull. No. 8* (1913).
3. J. E. Armstrong and W. L. Brown, *Geol. Soc. Amer. Bull.* **65**, 349–364 (1954).
4. D. J. Easterbrook, *Geol. Soc. Amer. Bull.* **74**, 1465–1484 (1963).
5. J. E. Armstrong, D. R. Crandell, D. J. Easterbrook, J. B. Noble, *Geol. Soc. Amer. Bull.* **76**, 321–330 (1965).
6. M. M. Leighton, *J. Geol.* **68**, 529–552 (1960).
7. J. C. Frye and H. B. Willman, *Geol. Soc. Amer. Bull.* **74**, 501–506 (1963).
8. G. M. Richmond, *Quaternary of the U.S.*, 7th INQUA Congr. Rev. Vol. (1965), pp. 217–230.
9. D. R. Mullineaux, H. H. Waldron, M. Rubin, *U.S. Geol. Survey Bull. 1194-0* (1965).
10. D. R. Crandell, *Quaternary of the U.S.*, 7th INQUA Congr. Rev. Vol. 353 (1965), pp. 341–353.

21 January 1966

## Trace Element Partition Coefficient in Ionic Crystals.

Abstract. *Partition coefficients of monovalent trace ions between liquids and either solid $NaNO_3$ or KCl were determined. The isotropic elastic model of ionic crystals was used for calculating the energy change caused by the ionic substitutions. The observed values of partition coefficients in KCl are in good agreement with calculated values.*

Recently, Masuda and Matsui (*1*) suggested a possible picture of the evolution of the earth's lithosphere on the basis of rare-earth element partition patterns. The theory requires a quantitative knowledge of trace element partition between crystallized minerals and their mother melts. The well-known Goldschmidt's rule, which predicts trace element partition qualitatively in terms of ionic radii, is not adequate for their purposes. Difference in chemical properties between elements complicates making the rule quantitative; but some simplified treatment could be applied to the series of chemically similar elements, provided that the difference between them in chemical properties is neglected. I now report the quantitative treatment of the trace element partition in one of the most idealized cases, that of the ionic crystals, based on the theory of lattice defects.

Table 1. Trace element partition coefficients in $NaNO_3$ and KCl.

| Element | Ionic radius* (Å) | Partition coefficient |
|---|---|---|
| | *$NaNO_3$* | |
| Na | 0.98 | (1) |
| Ag | 1.13 | $7.5 \times 10^{-1}$ |
| K | 1.33 | $2.5 \times 10^{-1}$ |
| Rb | 1.49 | $2.5 \times 10^{-2}$ |
| Cs | 1.65 | $4.8 \times 10^{-4}$ |
| | *KCl* | |
| K | 1.33 | (1) |
| Rb | 1.49 | $7.9 \times 10^{-1}$ |
| Cs | 1.65 | $3.4 \times 10^{-1}$ |

* Ionic radii given by Goldschmidt.

Table 2. Calculated and observed value of the energy change of trace element substitution in KCl. Theoretical values are calculated with use of ionic radii of Goldschmidt.

| Element | $\epsilon^2(1 + \epsilon/\gamma)$ | $U_{\text{calc.}}$ (cal/mol) | $U_{\text{obs.}}$ (cal/mol) |
|---|---|---|---|
| Rb | 0.014 | 500 | 510 |
| Cs | .060 | 2200 | 2300 |

Partition coefficients of trace amounts of Ag, K, Rb, and Cs in $NaNO_3$, and of Rb and Cs in KCl, between liquid (molten salt) and solid (crystal) phases have been determined by the method of partial crystallization or of zone melting.

Partition coefficients, except that of Ag in $NaNO_3$, were determined as follows. Reagent grade $NaNO_3$ or KCl was mixed with known amounts of trace material and packed in a Pyrex or quartz tube (about 1 cm in diameter). The tube was mounted in the furnace (Fig. 1*a*). The temperature of the furnace was controlled slightly above the melting point of the main component material. The tube was lowered at a rate of 0.001 to 3 cm per hour until a few tenths of the total liquid phase had crystallized. The crystallized portion comprised about one-tenth of the initial weight of the material for analysis. The Rb and Cs were analyzed by radioactive tracers, $Rb^{86}$ and $Cs^{137}$, and K was analyzed by frame photometry.

The partition coefficient of Ag in $NaNO_3$ is determined by the method of zone melting. The $NaNO_3$ is melted in a crucible and poured into a Pyrex tube. A small amount of $AgNO_3$ is placed above the $NaNO_3$ in the tube. The molten zone (about 1 cm) produced by a small ring heater was moved from top to bottom at a rate of 0.3 to 3 cm per hour. The crystal Ag in $NaNO_3$ thus formed was analyzed by ethylenediaminetetraacetate titration on each piece of crystal, cut to about 1 cm long. The partition coefficient is calculated from the slope of the straight line in Fig. 2.

The partition coefficients of Ag, K, Rb, and Cs in $NaNO_3$ are independent of the rate of crystal growth below 0.3 cm/hr (Fig. 3). The partition coefficients of Rb and Cs in $NaNO_3$ are constant for variations of the trace ion concentration below $10^{-2}$ and $10^{-4}$ mol/mol, respectively (Fig. 4). At higher concentrations, reproducible values of the partition coefficients have not been obtained. The observed values of the partition coefficients in KCl and $NaNO_3$ decrease regularly with increasing ionic radius (Table 1).

In order to calculate the partition

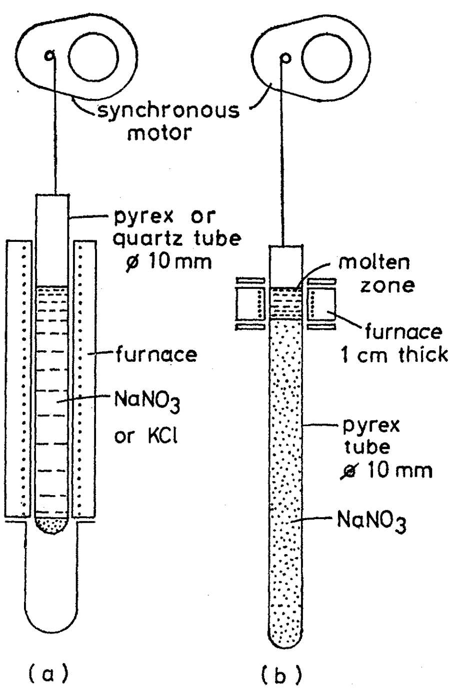

Fig. 1. Apparatus for determining partition coefficients. Arrangement of furnace and column for (*a*) partial crystallization and (*b*) zone melting.

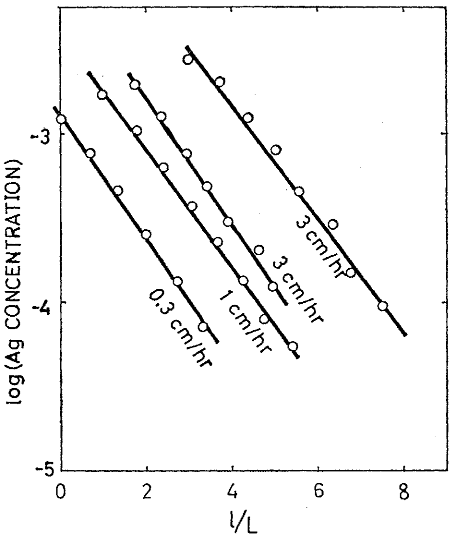

Fig. 2. Silver concentration plotted against *l/L*, where *L* is the width of molten zone, *l* is the position of the piece of crystal measured from the upper end. *D* is calculated from the equation $\log(C/C_0) = 0.4343 \cdot D(l/L)$, where *C* and $C_0$ are the concentrations of Ag at 1 and 1 = 0, respectively.